

UNIVERSITY OF LATVIA
FACULTY OF PHYSICS AND MATHEMATICS



Aleksandrs Kalinko

**INTERPRETATION OF X-RAY
ABSORPTION SPECTRA USING
MOLECULAR DYNAMICS SIMULATIONS**

Summary of Doctoral Thesis

Promotion to the Degree of Doctor of Physics
Subbranch: Solid State Physics

Riga 2012



This work has been supported by the European Social Fund within the project Support for Doctoral Studies at University of Latvia

Type of the thesis: **Doctoral thesis**

Scientific advisor: *Dr. phys.* **Aleksejs Kuzmins**

Reviewers:

Dr. phys. **Vyacheslavs Kashcheyevs**, senior researcher, University of Latvia

Dr. habil. phys. **Donats Millers**, senior researcher, Institute of Solid State Physics, University of Latvia

Dr. Francesco Rocca, senior researcher, Bruno Kessler Foundation (FBK) and Institute for Photonics and Nanotechnologies (IFN) of the National Research Council (CNR)

The defense of the doctoral thesis will take place in an open session of the Promotion Council of Physics, Astronomy and Mechanics of the University of Latvia on the **23th of March, 2012, at 15:00** in the conference hall of the Institute of Solid State Physics, University of Latvia.

The doctoral thesis and its summary are available at the Library of the University of Latvia (4 Kalpaka Blvd, Riga) and Latvian Academic Library (10 Rupniecibas Srt, Riga).

Chairperson of the Specialized Promotion Council of the scientific section of the Physics, Astronomy and Mechanics at the University of Latvia: *Dr. habil. phys.* **Ivars Tale**.

© Aleksandrs Kalinko, 2012

© University of Latvia, 2012

ISBN 978-9984-45-449-8

Abstract

The x-ray absorption spectroscopy is widely used structure determination technique, which is highly sensitive to the local structure. However, the nowadays extended x-ray absorption fine structure (EXAFS) spectra analysis meets complications due to the presence of multiple scattering effects and thermal disorder. In this work we have developed the method of the EXAFS spectra analysis based on the quantum mechanics-classical molecular dynamics approach coupled with ab-initio EXAFS spectra calculations. The method allows one to obtain unique information on the local atomic static and dynamic structure in crystalline materials, through the analysis of the many-atom distribution functions at required temperature and pressure. The method was applied to the modelling of the EXAFS spectra from crystalline ReO_3 , CaWO_4 and ZnWO_4 . The investigation of nanocrystalline ZnWO_4 is also reported.

Contents

1. Introduction	5
1.1. Motivation	5
1.2. Aim and objectives of the work	7
1.3. Scientific novelty of the work	8
1.4. Author's contribution	9
2. X-ray absorption spectra analysis using molecular dynamics	10
2.1. Basics of X-ray absorption	10
2.2. EXAFS spectra analysis using molecular dynamics simulations	13
2.3. Ab initio calculation of configuration averaged EXAFS	17
3. Experimental	20
3.1. Samples and characterization	20
3.2. X-ray absorption spectroscopy	20
4. Results	22
4.1. Local structure in ZnWO ₄ nanoparticles	22
4.2. MD-EXAFS data analysis	24
4.2.1. Application to ReO ₃ crystal	24
4.2.2. Application to CaWO ₄ crystal	26
4.2.3. Application to ZnWO ₄ crystal	27
5. Conclusions	30
Main theses	34
References	35
Author's publication list	40
Participation in conferences	41
Participation in schools with posters	43

1

Introduction

1.1 Motivation

The knowledge of the atomic structure is crucial to understand physical and chemical properties of any material. It provides a starting point for computer simulation studies in condensed matter physics, which play nowadays a fundamental role in many areas of investigation. Among different simulation techniques, quantum mechanical calculations, Monte Carlo and molecular dynamics simulations are today the most popular methods allowing one a detailed access to the static and dynamic properties of the material in a phase space [3].

While a number of experimental techniques probing structure related properties is rather large, there are only two *direct* structural tools, namely *x-ray (neutron/electron) diffraction* and *x-ray absorption spectroscopy*, which provide complementary information on the static and dynamic structure of a material.

In the diffraction experiment for polycrystalline solid, the Bragg reflections are measured, and then the atomic structure is solved using the Rietveld method [41]. The structure of polycrystalline solid is described by a symmetry group and a small number of structural parameters, known as the lattice parameters. Note that the diffraction experiments include also information on the thermal atomic motion allowing one to estimate the mean amplitude of atom vibrations, described by the *mean-square displacement* (MSD) parameter.

Since the Bragg peaks appear only in the case of periodic structures, another approach is used for the disordered solids, such as glasses and amorphous materials. In

this case, the experimental scattering signal due to the elastic interaction between radiation and the solid includes only diffuse scattering. An intermediated situation can occur in nano-materials, where both diffuse and Bragg scattering can be present simultaneously. Therefore, the short and intermediate range order structure in such materials is determined from the analysis of the total scattering data using the Fourier transformation (FT) technique [37]. As a result, the atomic pair distribution function (PDF) is obtained, which shows the probability to find a pair of atoms separated by some distance. Opposite to diffraction, the contribution of the thermal atomic motion to PDF is described by the *mean-square relative displacement* (MSRD) parameter, which shows a variation of the interatomic distance.

The synchrotron-based x-ray absorption spectroscopy (XAS) is a powerful and versatile experimental technique to probe the local electronic and atomic structure of the materials [40]. The method is element specific, being well adapted for complex compounds, and is not limited by the state of the sample, so gases, liquids and solids can be studied equally well [12, 18]. Using focused x-rays, XAS allows one to study the local atomic structure around the absorbing atom at macro, micro- and nano-scale [18]. Time-resolved *in situ* XAS studies are also routinely possible in the range from minutes down to milliseconds, also under extreme conditions, such as high pressure and/or high temperature [7, 35]. X-ray absorption spectrum contains information on the many-atom distribution functions and, thus, is sensitive to the 3D structure of the material. However, due to a complexity of the problem, until now its practical application was mainly limited to the determination of near-neighbor distances, coordination numbers, static and thermal MSRDs, bonds anharmonicity, and ion oxidation states.

Some examples of XAS applications include the following. Being structurally local technique, the XAS is widely used for investigation of hydration structure of different ions in solutions [11]. The structural aspects of glasses are also studied by elucidating the structural role of the selected ions [23]. One can also probe the homogeneity of dopants in a glass and to check clustering effect depending on dopant concentration [2, 10]. Note that no other direct structural methods can provide such information. XAS is also suitable for the investigation of phase transitions induced by pressure or temperature [27, 52] and watching in-situ chemical reactions [17]. So, the application of XAS in different areas of physics and chemistry can be undoubtedly helpful to solve many practical tasks.

The experimental x-ray absorption spectra are conventionally divided into two parts: the x-ray absorption near edge structure (XANES), which is located up to about 50 eV above the Fermi level and includes electronic effects, and the extended x-ray absorption fine structure (EXAFS), which extends up to about 2000 eV above the Fermi level and includes local structural information around the absorbing atom. In this thesis only the EXAFS part is considered.

While general theory of the EXAFS has been developed in the past [40], the conventional analysis procedure of the EXAFS spectra is reliably defined only for the first coordination shell of the absorbing atom. It accounts only for the contributions from the pair atom distributions, known as the *single-scattering* (SS) effects. The same analysis of the further coordination shells is also possible, but only when the contribution from the many-atom distributions, known as the *multiple-scattering* (MS) effects, are negligible. While such requirement is strictly speaking never fulfilled, however the neglect of the MS contributions can be still a good approximation in some cases [39].

In general case, more advanced analysis of the full EXAFS spectrum, accounting for the multiple-scattering effects, should be used. Such computer codes are available today [13, 14, 40], however they are able to perform simulations either for a static atomic configuration or to account for the thermal atomic motion through simple analytical approximations such as the Einstein or Debye models. One should point out that thermal disorder significantly affects the EXAFS spectrum, being usually responsible for up to 20-80% of the total amplitude. Therefore, the accurate accounting of the thermal atomic motion in the EXAFS spectra is crucial for the analysis but still remains an unresolved issue.

The possible solution of this problem is to use the molecular dynamics (MD) or Monte Carlo (MC) simulations in a combination with ab initio EXAFS calculations. Both methods allow starting from an interaction potential model to obtain a set of atomic configurations, which can be used further to calculate the configuration-averaged EXAFS signal at required experimental conditions (temperature, pressure).

1.2 Aim and objectives of the work

The research activities underlying the thesis include both experimental (sample synthesis and studies by several experimental method including experiments at synchrotron

facility) and theoretical (software development and computer simulations) work.

The main goal of the present work is to further develop the method for the EXAFS spectra modelling based on the quantum mechanics-classical molecular dynamics (QMMD) approach coupled with ab initio EXAFS spectra calculations. The method allows one to obtain unique information on the local atomic static and dynamic structure in crystalline materials, through the analysis of the many-atom distribution functions at required temperature and pressure.

The advantage of the method is its ability to accurately account for thermal disorder within the multiple scattering (many-atom) effects that allows one to perform direct simulation of the total EXAFS signal. Note that the use of classical molecular dynamics limits our analysis to the high-temperature region, however such limitation is not inherent for the method itself and can be overcome by using the quantum MD.

The objectives of the present work are to demonstrate

- the potentiality of the method for the analysis of experimental EXAFS spectra on an example of crystalline systems with the different local coordinations. The three studied compounds ReO_3 , CaWO_4 and ZnWO_4 cover different types of $5d$ -element (W, Re) local coordination, starting from regular tetrahedral in tetragonal CaWO_4 to distorted octahedral in monoclinic ZnWO_4 , and, finally, regular octahedral in cubic perovskite-type ReO_3 .
- the ability of the EXAFS technique to deal with highly distorted local atomic structure on an example of nano-crystalline ZnWO_4 , having large surface to bulk ratio.

1.3 Scientific novelty of the work

The study of the local atomic structure (up to $\sim 6 \text{ \AA}$ around the absorbing atom) in ReO_3 , CaWO_4 and ZnWO_4 crystals has been performed by x-ray absorption spectroscopy (EXAFS) simultaneously taking into account thermal disorder and multiple-scattering (many-atom) effects within the QMMD-EXAFS approach.

Significant deformation of the local atomic structure around W and Zn atoms in nano-crystalline ZnWO_4 has been determined by the EXAFS technique in comparison with the micro-crystalline zinc tungstate. The complementary studies by EXAFS and

Raman spectroscopy allowed us to conclude that the $[\text{WO}_6]$ octahedra deformation in nano-crystalline ZnWO_4 results in the formation of short double tungsten-oxygen bonds.

1.4 Author's contribution

The major part of the work has been done at the Institute of Solid State Physics, University of Latvia. The XAS measurements were performed at HASYLAB (Hamburg, Germany) using synchrotron radiation produced by the DORIS III storage ring. The author has been participating in the nano-samples synthesis, their characterization by the IR and Raman spectroscopy, temperature dependent EXAFS measurements of nano and microcrystalline ZnWO_4 and CaWO_4 . The quantum mechanical calculations, analysis of the experimental EXAFS data and the advanced modelling of EXAFS spectra have been performed by the author at the Latvian SuperCluster facility [22]. The computer code for the force-field potential parameters optimization has been also developed by the author based on the simulated annealing method.

The results of this work have been presented at 9 international conferences and 4 international schools during 2008-2011 and discussed at the scientific seminar at the Institute of Solid State Physics, University of Latvia on May 09, 2011. Main results have been published in 7 SCI papers.

X-ray absorption spectra analysis using molecular dynamics

2.1 Basics of X-ray absorption

The x-ray interaction with matter occurs elastically (coherent), when the kinetic energy of the incident photon is conserved, and inelastically (incoherent), when the kinetic energy of the incident photon is not conserved. In an inelastic scattering process, some of the energy of the incident photon is lost or gained. There are three types of the inelastic x-ray interactions with matter: the photoexcitation of electrons, the Compton effect and the electron-positron pair production.

In Fig. 2.1 photon cross-section dependance on the excitation energy for W atom is shown. In the hard x-ray range (~ 10 keV) photoexcitation process dominates, therefore the assumption that x-ray absorption coefficient is proportional to the photoexcitation transition rate can be made.

In x-ray absorption spectroscopy experiments, the absorption of x-rays by the sample with thickness (d) is measured as a function of x-ray energy. The x-ray absorption coefficient $\mu(E)$ is determined by measuring the incident (I_0) and transmitted (I) x-ray beams intensities as

$$\mu(E) = \frac{1}{d} \ln\left(\frac{I_0}{I}\right). \quad (2.1)$$

The energy dependence of the x-ray absorption coefficient (Fig. 2.2) shows three main features: when photon energy increases, the absorption coefficient decreases before an absorption edge, at certain energy the sharp change of the absorption coefficient

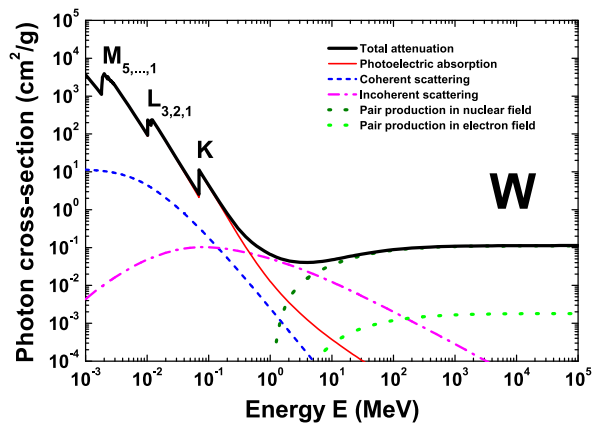


Figure 2.1: Photon cross-section components and total attenuation for tungsten atom. K, L and M are the absorption edges due to the electron transitions from the core levels.

occurs and is called the edge, and, finally, the oscillating variation of the absorption coefficient occurs above the edge. These oscillations are called the extended x-ray absorption fine structure (EXAFS). The EXAFS signal $\chi(E)$ is defined as the normalized, oscillatory part of the x-ray absorption coefficient (μ) above a given absorption edge

$$\chi(E) = \frac{\mu(E) - \mu_0(E) - \mu_b(E)}{\mu_0(E)} \quad (2.2)$$

where $\mu_b(E)$ is the background absorption coming from electrons of the outer shells, and $\mu_0(E)$ is the atomic-like contribution. The fine structure, i.e. EXAFS, arises due to the scattering of the excited photoelectron by a potential from all neighbouring atoms surrounding the absorbing atom. The photoelectron is excited into empty states above the Fermi level, and its lifetime is limited by the lifetime of the core-hole and by an interaction with other electrons. The photoelectron lifetime restricts its mean free path and, thus, is responsible for the local sensitivity of the method. Therefore, the EXAFS signal probes the local structural and electronic information around the absorber.

Interpretation of the EXAFS signal gives detailed information about local atomic structure (distance to the nearest neighbouring atoms, neighbouring atoms count, thermal and static disorder). Conventional EXAFS data analysis is based on the separation of the EXAFS signals for different coordination shells and their independent analysis.

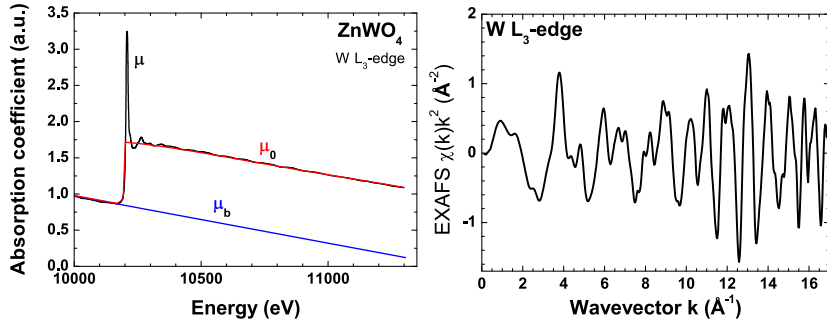


Figure 2.2: (left panel) The experimental x-ray absorption spectrum (μ) of the W L_3 -edge in ZnWO_4 . μ_b is the background contribution, μ_0 is the atomic-like contribution. (right panel) EXAFS oscillations $\chi(k)k^2$ extracted from the experimental absorption coefficient shown in left panel.

The Fourier transform (FT) and back-Fourier transform (BFT) are used for this operation. The FT converts EXAFS signal from k -space to R -space, where one can see the regions, which correspond to the different coordination shells. Next, one chooses the region corresponding to the single coordination shell in R -space and, by performing BFT, obtains the isolated EXAFS signal in k -space. This signal is further used for the modelling. The most common technique is a parametrization of the signal within the so-called Gaussian or cumulant model [15]. Another possibility is to reconstruct the radial distribution function (RDF) using, for example, regularization technique [29]. In most cases, the accurate analysis can be performed only for the region of the first coordination shell of the absorber, where the multiple-scattering effects do not exist. In some special cases, when the multiple-scattering contributions into the EXAFS signal can be neglected, it is also possible to extend the analysis to the further (outer) coordination shells.

Previously described methods are valid for the first coordination shell and the outer coordination shells, when they do not overlap with the multiple-scattering contributions. However, in most practical cases the multiple-scattering effects give strong influence on the EXAFS signal after the first coordination shell. Another important point is to account for static and thermal disorder in a material. Even in the case of crystalline material, where atomic positions are strictly defined, the conventional analysis of the

full EXAFS spectrum including thermal disorder is complicated and often impossible. This is due to a number of fitting parameters required to describe correlated motion of atoms for each scattering paths. For highly disordered materials as glasses or liquids, the problem becomes even more complicated.

To overcome these problems, the advanced technique exists which combines molecular dynamics or Monte-Carlo simulations with either conventional EXAFS spectra analysis or ab initio EXAFS spectra calculations.

In the literature many different combinations of advanced EXAFS spectra analysis can be found. The big part of the works is dedicated to the analysis of the local structure in glasses [6, 21, 34, 43, 49, 50]. Another part of works considers local structure of metal ions in solutions [20, 32, 46, 47] or liquid materials [31, 36, 51]. In recent years, works dedicated to the local structure investigation by EXAFS and MD in monoatomic and more complex solids become popular [5, 8, 24, 25, 26, 30, 33, 36, 42, 44, 48].

2.2 EXAFS spectra analysis using molecular dynamics simulations

The today difficulties of the EXAFS analysis are mainly connected to the two problems. The first one is an account for the photoelectron multiple-scattering (MS) effects, which contribute into the EXAFS spectra analysis beyond the first coordination shell in R -space. The second problem is related to an account for thermal and static disorder, especially, within the MS contribution.

One should note that when the size of the system grows up, the use of simple Gaussian/cumulant models becomes unpractical, due to a huge number of fitting parameters is required. Considering all MS contributions independently, each scattering path is described by at least three parameters, i.e. path degeneracy, length and MSRD. Therefore, an increase of the EXAFS spectrum analysis interval ΔR in R -space leads to the exponential growth of the number of scattering paths as well as of the fitting parameters. At the same time, the maximum number of fitting parameters is limited, according to the Nyquist theorem

$$N_{exp} = \frac{2\Delta k\Delta R}{\pi} + 2, \quad (2.3)$$

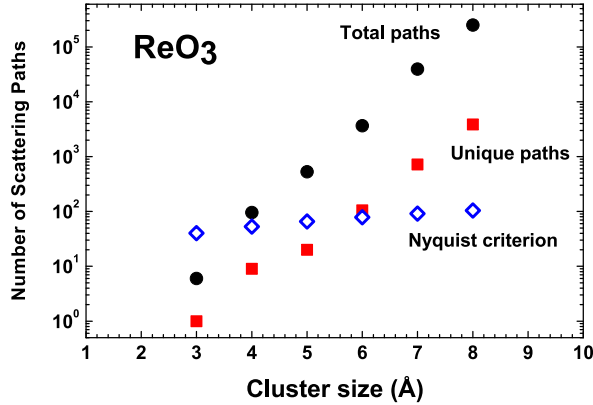
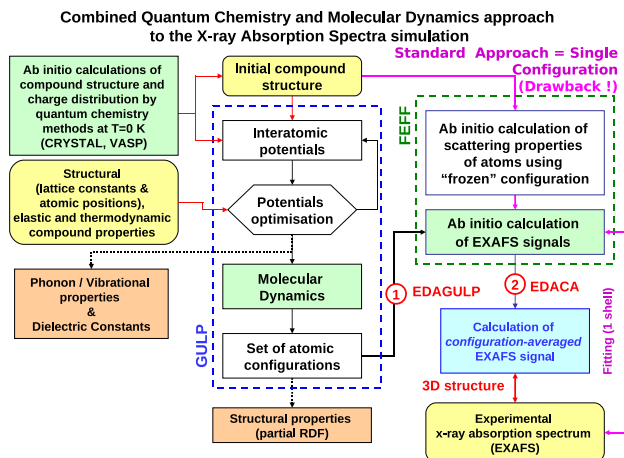


Figure 2.3: The dependence of the number of scattering paths on the cluster size for ReO_3 .

by the number of independent points (N_{exp}) in the experimental signal given in the k -space interval Δk .

The dependence of the number of scattering paths on the cluster size is shown in Fig. 2.3 for ReO_3 as an example. Here the circles and squares represent the total number and the unique number of scattering paths, respectively. The number of the unique paths is much smaller than their total number due to the crystal symmetry. However, the crystal symmetry becomes broken when thermal or static disorder is introduced, i.e. when atoms are randomly displaced from their equilibrium positions. In this case, all scattering paths must be considered. The diamonds in Fig. 2.3 indicate the number of independent experimental data points according to the Nyquist theorem. Δk was chosen equal to 20 \AA^{-1} , that corresponds to the high-quality data obtained at modern experimental setups. According to the results reported in Fig. 2.3, the analysis of the EXAFS signal in ReO_3 becomes impractical beyond 6 \AA even when some analytical model for the thermal vibrations, which reduces the total number of fitting parameters, is used. In many closed packed structure with low crystal symmetry this range will be much smaller.

Another problem related to the thermal disorder is its impact on the EXAFS signal amplitude through the variation of the path geometry. This influence is twofold. First, the thermal vibrations will lead to the EXAFS signal damping at high k -values.



Second, they will modify the scattering path geometry and, thus, directly influence the scattering amplitude and phase of the multiple-scattering signals. Note that even if the thermal displacements of atoms are rather small, the non-linear angular dependence of the multiple-scattering signals can result in an appreciable change of the EXAFS signal [28].

To overcome the above mentioned problems, the following approach can be adapted. The time-dependent dynamics of the system can be approximated by a set of atomic configurations (snapshots), taken at short periods of time. The sampling time is strictly connected to the highest characteristic frequency of the compound and is usually located in the femtoseconds range (0.5 fs in the present work). Since each snapshot represents the static atomic configuration, its EXAFS signal can be easily calculated including rigorously all multiple-scattering contributions. Next, the configuration-averaged EXAFS signal is determined by averaging over all snapshots, thus accounting for the dynamic disorder.

For practical realization of the method, a combination of molecular dynamics simulation and ab initio EXAFS calculations can be used. Molecular dynamics simulation produces a set of atomic configurations at required temperature and pressure, thus introducing the disorder. The ab initio EXAFS calculations allow one to accurately

evaluate the EXAFS signal for static configuration, thus accounting for the multiple-scattering effects.

In the Fig. 2.4 the general MD-EXAFS simulation scheme [25, 26] is shown. It combines three calculation methods, quantum chemistry, classical molecular dynamics (MD) and ab initio EXAFS calculations.

One should point out that a number of important approximations are employed when doing the MD simulations. First, the use of the Born-Oppenheimer or adiabatic approximation allows one to separate treatment of electrons and nuclei. As a result, for each set of nuclear positions, one can get the energy contributed by the electrons. This energy together with the nuclear-nuclear repulsions determines the total potential energy and can be used to find the forces acting on the atoms. One can introduce the potential energy surface by requiring that the total potential energy is a function of atomic positions only, thus eliminating the electrons from the consideration. Next, the nuclei are treated as classical particles moving on the potential energy surface, thus replacing the Schrödinger's equation with the Newton's one. Finally, the potential energy surface is approximated by an analytical function (force-field) that gives the potential energy and interatomic forces as a function of atoms coordinates.

The starting point of the analysis is the compound structure, which can be determined for crystalline compounds from diffraction experiments. The structural information and other physical properties give an idea for choosing the type of the force-field model, i.e. the interaction potentials between atoms. Once interatomic potentials are defined, the optimization procedure can be performed to obtain potential parameters, which reproduce best structure and given properties. Further, the MD simulations are performed using the obtained force-field model to get a set of atomic configurations.

The results of the MD simulations allow one to make some conclusions about correctness of interatomic potentials. The total and partial RDF functions can be calculated and compared with the first coordination shell RDFs obtained from the conventional EXAFS data analysis. Additionally the average atomic positions can be compared with initial structure to check whether there is strong atoms displacements or not. The strong displacements of atoms from the equilibrium positions indicate the problem with the FF model.

After performing the MD simulations, every single atomic configuration is used to calculate the EXAFS signal. Finally, the configuration averaged EXAFS signal is

calculated and directly compared with the experimentally measured EXAFS spectrum.

At the potential parameters optimization step, the experimentally measured properties can be complemented with that calculated by quantum chemistry methods. The best example is the phonon dispersion relations through the first Brillouin zone. For the most materials, it is relatively easy to measure vibrational frequencies at the Γ point of the Brillouin zone using Raman and/or infra-red spectroscopy. However, the measurement of the phonon dispersion relations is a complicated experimental task, which can be performed only at large scale facilities exploiting neutrons or x-ray synchrotron radiation and requires the availability of monocrystalline sample [16]. At the same time, the knowledge of phonon dispersion relations helps to make the force-field optimization procedure more reliable and stabilizes the solution.

2.3 Ab initio calculation of configuration averaged EXAFS

The MD simulation provides with a set of atomic configurations. Each single configuration describes a static state of the system at some moment of time. The set of such configurations can be used to calculate properties depending on the atomic coordinates. In the case of EXAFS, each static atomic configuration is used to calculate single EXAFS spectrum taking into account all multiple-scattering contributions. Since each atomic configuration is static, there is no need to introduce the disorder effects in the multiple-scattering formalism. Finally, the configuration averaged EXAFS signal, inherently including thermal and static disorder, is calculated as

$$\chi(k) = \frac{1}{N_t} \sum_{t=1}^{N_t} \left(\sum_n \sum_j \frac{N_j f_j^n(k, t)}{k R_j^2(t)} \sin[2k R_j(t) + \delta_j^n(k, t)] \right) \quad (2.4)$$

where n is the multiple-scattering order (single-scattering, double-scattering, triple-scattering, etc.), j is the atomic group number, N_j is the degeneracy of the scattering path involving atom(s) of the j -group, $2R_j(t)$ is the scattering path length, $f_j^n(k, t)$ and $\delta_j^n(k, t)$ are the scattering amplitude and total phase shift functions. The "time" variable t indicates the number of the atomic configuration in the MD simulation. N_t is the total number of atomic configurations.

For the accurate simulation of the EXAFS spectra, the set of atomic configurations should fulfill some conditions.

The first is the number of configurations, which is proportional to the time of the MD simulation. The characteristic time of the photoabsorption process is in the range of 10^{-15} - 10^{-16} seconds. The characteristic time of the atomic vibrations is much longer being in the range of 10^{-13} - 10^{-14} seconds. This means that a single photoabsorption process sees "frozen" atomic structure. However, the time of the EXAFS experiment is in the range of minutes, and, thus, the resulting EXAFS signal equals to a superposition of EXAFS signals from many static configurations. Therefore, for a solid, where atoms move close to their equilibrium positions, the simulation time should be larger than the characteristic time of the atomic vibrations. Ideally, one should choose the number of atomic configurations enough large to have the average over the statistical ensemble in the MD simulation close to the average over time in the experiment. In this work, the number of atomic configurations used in the calculation of the averages was at least 4000. Moreover, the convergence of both the average atomic structure and the average EXAFS signal were controlled.

The second condition is that the time step in the MD simulation should be enough small to sample correctly the highest characteristic frequency of the material and to guarantee accurate integration of the equations of motion, thus resulting in a smooth trajectory for all atoms. The highest characteristic frequency of the material can be estimated either experimentally from the Raman or IR spectra as well as from inelastic scattering experiments or theoretically from lattice dynamics calculations. In this work, the estimated time step of 0.5 fs was used.

The third condition is the size of the MD simulation box. In the simulations of solid materials the periodic boundary conditions are used. This leads to the correlations between atomic movements at distances larger than the size of the box. Therefore, the calculation of EXAFS signal without artificial correlations is possible only at distances smaller than half of the box dimensions. For example, to analyse structural contributions in the EXAFS signal till 6 Å the size of the MD simulation box should be at least 12 Å in all dimensions.

Another important note should be made regarding the computer code, which is used to calculate EXAFS signal for the static configuration. In this work we use the ab initio real-space multiple-scattering FEFF8.x code [4, 40], thus the EXAFS signals are

calculated taking into account all multiple scattering contributions to the eighth order. The number of the multiple-scattering paths increases roughly exponentially with the box size, thus arriving rapidly to the maximum number of paths, which can be treated by the FEFF code due to the computer memory limitations. Of course, the MS paths number varies depending on the material. In this work, for all crystals we were able to calculate the configuration averaged EXAFS signals for the cluster sizes of at least 6 Å.

Experimental

3.1 Samples and characterization

ReO₃ and CaWO₄ commercial polycrystalline powder with 99.9% purity were used in this work. ZnWO₄ nano- and polycrystalline powders were synthesized by co-precipitation technique.

Samples characterization were performed by x-ray diffraction, infra-red, Raman and photoluminescence spectroscopies. X-ray absorption measurements were performed for CaWO₄ and ZnWO₄ samples.

3.2 X-ray absorption spectroscopy

X-ray absorption measurements were performed in transmission mode at the HASY-LAB DESY C1 bending-magnet beamline (Fig. 3.1) in the temperature range of 10-300 K at Zn K (9659 eV) and W L₃ (10207 eV) edges. The storage ring DORIS III was used as an x-ray source. It operated at $E=4.44$ GeV and $I_{max}=140$ mA in a 5 bunches mode with a lifetime of 4 h. The higher-order harmonics were effectively eliminated by detuning of the monochromator Si(111) crystals to 60% of the rocking curve maximum, using the beam-stabilization feedback control. The x-ray beam intensity was measured by three ionization chambers filled with argon and krypton gases.

The Oxford Instruments liquid helium flow cryostat was used to maintain the required sample temperature. The temperature was stabilized to within ± 0.5 degrees during each experiment. Several samples of ZnWO₄ and CaWO₄ were prepared by depositing an appropriate amount of the powder on Millipore filters and fixing by a

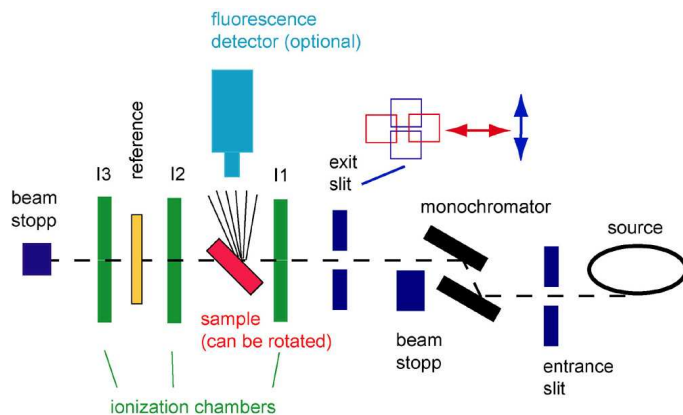


Figure 3.1: Schematic view of the EXAFS experiment at C beamline DORIS III storage ring. The setup consists of the x-ray source (the storage ring), variable entrance and exit slits, double-crystal monochromator, three ionization chambers (I1, I2, and I3), beam stopper. The position of the unknown and reference samples and the optional fluorescence detector (not used in the present work) are also shown [1].

Scotch tape. The deposited powder weight was chosen to give the absorption edge jump value $\Delta\mu_x \simeq 1.0$ at the Zn K or W L₃ edges. The tungsten foil was used as the reference sample to control monochromator stability.

Experimental temperature-dependent EXAFS spectra for the Re L₃-edge in polycrystalline ReO₃ were taken from [38].

Results

4.1 Local structure in ZnWO_4 nanoparticles

Nanoparticles and microcrystalline ZnWO_4 were studied by temperature dependent x-ray absorption spectroscopy at the Zn K and W L_3 -edges. The obtained results were compared with that determined by complementary experimental techniques as x-ray powder diffraction, Raman and photoluminescence spectroscopies allowing us to probe different aspects of the local atomic and electronic structure.

It was found that the observed changes in the optical properties and lattice dynamics of ZnWO_4 nanoparticles cannot be attributed only to the size reduction, but are related to the relaxation of their atomic structure, including formation of surface defects.

The presence of strong structural relaxation in ZnWO_4 nanoparticles was confirmed by x-ray absorption spectroscopy study. In the Fig. 4.1 experimental EXAFS spectra temperature dependence and corresponding Fourier transformations are shown for both W L_3 and Zn K edges. The independent analysis of the EXAFS signals at the W L_3 and Zn K edges by the model-independent approach allowed us to reconstruct the first coordination shell RDFs (Fig. 4.2) and to follow their temperature variation. The significant distortions of the $[\text{WO}_6]$ and $[\text{ZnO}_6]$ octahedra, directly observed in ZnWO_4 nanoparticles by EXAFS, show only minor temperature dependence. The distortion results in the shortening of the metal-oxygen (W-O and Zn-O) bonds to the nearest oxygen atoms and the formation of the W=O bonds, whereas the longest bonds are elongated and becomes weaker.

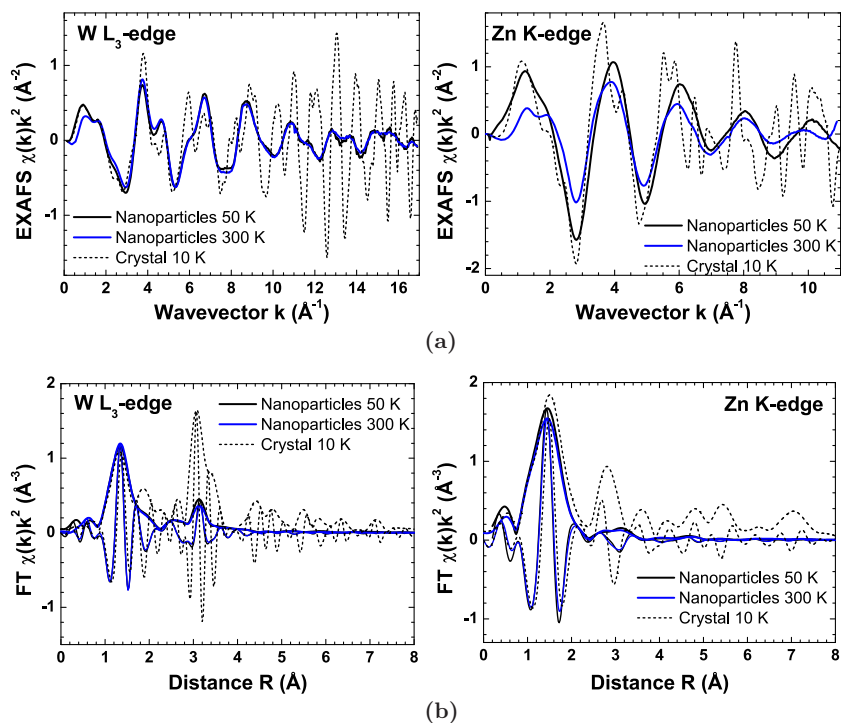


Figure 4.1: (a) Experimental W L₃-edge and Zn K-edge EXAFS spectra $\chi(k)k^2$ of nanoparticles and microcrystalline ZnWO₄. Only representative signals are shown for clarity. (b) Fourier transforms of the experimental W L₃-edge and Zn K-edge EXAFS spectra $\chi(k)k^2$ of nanoparticles and microcrystalline ZnWO₄. Both modulus and imaginary parts are shown. Only representative signals are shown for clarity.

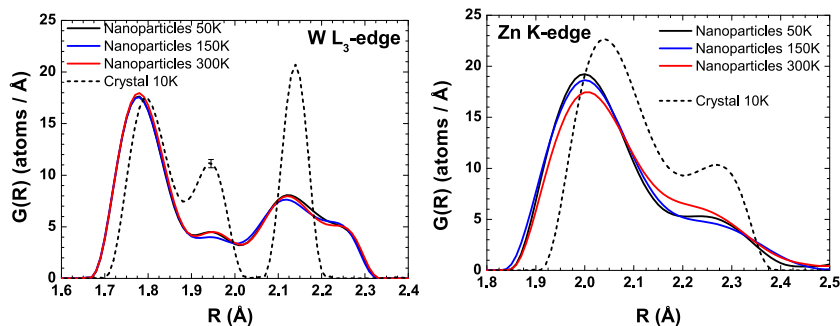


Figure 4.2: The reconstructed RDFs $G(R)$ for the first coordination shell of tungsten and zinc in nanoparticles and microcrystalline ZnWO_4 at representative temperatures. See text for details.

4.2 MD-EXAFS data analysis

4.2.1 Application to ReO_3 crystal

ReO_3 was chosen as an example for the MD-EXAFS method application due to its relatively simple highly-symmetric atomic structure, which is described by only one structural parameter. This allowed us to develop simple force-field model and to use classical molecular dynamics method. Quantum mechanical LCAO calculations were additionally used to determine physical properties of ReO_3 , being not available from experiments. The main achievement of using LCAO calculations was phonon dispersion curves (Fig. 4.3) which were further used for fine force-field model tuning.

Using the developed force-field model, the MD simulations were performed at three different temperatures. The MD simulation results were used to calculate dynamical properties of ReO_3 . In particular, the anisotropy of the oxygen atoms thermal vibrations was confirmed (Fig. 4.4 left panel), and the temperature dependence of the Re–O–Re bond angle distribution (Fig. 4.4 right panel) was determined.

It was shown that the calculated configuration averaged EXAFS signals agree well with the experimental ones at all temperatures. It was also shown that the analysis of the EXAFS signals from the outer coordination shells located at distances larger than 2 Å requires consideration of the MS effects (Fig. 4.5), which overlap strongly with the pair-wise EXAFS contributions.

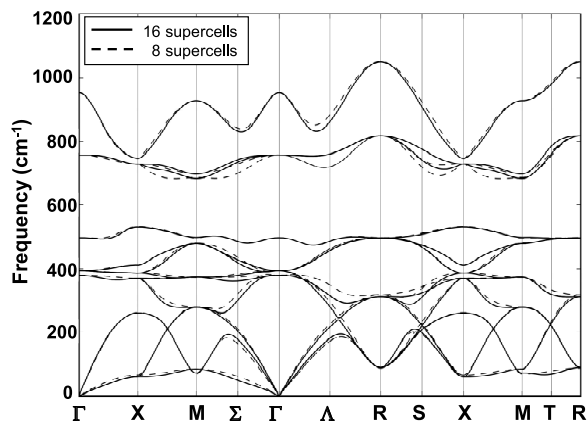


Figure 4.3: Phonon dispersion curves calculated by LCAO method.

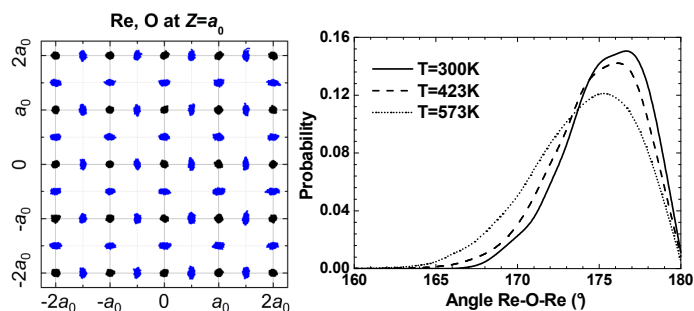


Figure 4.4: (left panel) Representation of MD trajectories at 573 K for Re (black) and O (blue) atoms located in a plane $Z = a_0$ (a_0 is the lattice parameter). (right panel) Distribution of the Re-O-Re angles at 300 K, 423 K and 573 K, calculated from MD simulations.

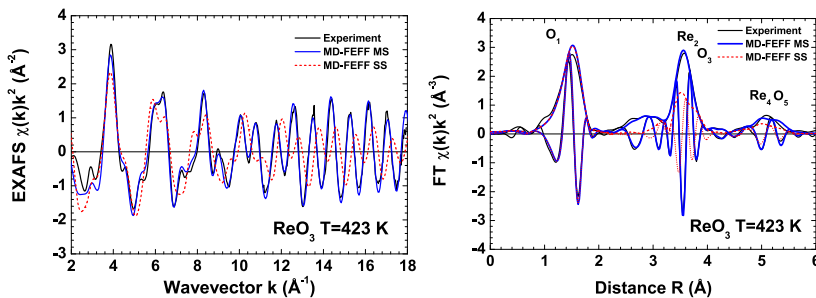


Figure 4.5: Results of the Re L_3 -edge EXAFS modelling in ReO_3 using MD-EXAFS method within the SS and MS approximation: (left panel) EXAFS signals and (right panel) corresponding Fourier transforms.

4.2.2 Application to CaWO_4 crystal

Ab initio calculations of the structural and electronic properties of scheelite-type CaWO_4 crystal have been performed within the periodic LCAO method using hybrid Hartree-Fock-DFT theory. The obtained results are in good agreement with known experimental data, including vibrational properties probed by Raman and infra-red spectroscopies. The QM calculations were also used to obtain charges on atoms.

The two force-field models [9, 45] were used in the MD simulations performed at 300 K. The Cooper model [9] was re-optimized to provide the difference between experimental and calculated structural parameters of about $\pm 0.01 \text{ \AA}$. As a result of the MD simulations, both models gave similar RDF functions. However, the comparison of the configuration averaged EXAFS signals with the experimental W L_3 -edge EXAFS spectrum allows us to conclude for benefit of the Senyshyn FF model. Therefore, it was finally used to study the influence of the MS effects on the EXAFS signal.

It was found that the MS contributions have minor influence on the W L_3 -edge EXAFS signal in CaWO_4 (Fig. 4.6). The main part of the EXAFS signal comes from oxygen atoms in the first coordination shell. Besides, there is also noticeable contributions from the outer group of oxygen atoms located till 5 \AA and from Ca atoms at 3.79 \AA (Fig. 4.7). The contribution from the heavy tungsten atoms, located at about 3.88 \AA is surprisingly small due to the thermal disorder (Fig. 4.7).

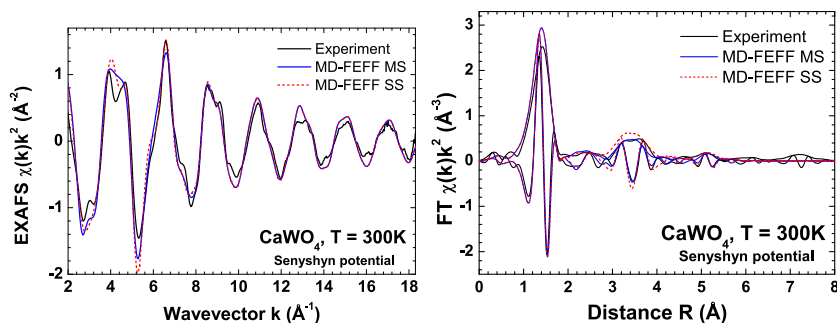


Figure 4.6: Results of EXAFS modelling using MD-EXAFS method for Senyshyn force-field potential model. (left panel) W L₃-edge EXAFS signal in CaWO₄, (right panel) FT of the W L₃-edge EXAFS signal in CaWO₄. The configuration averaged EXAFS signals containing only SS (MD-FEFF SS) or all MS (MD-FEFF MS) contributions are shown.

4.2.3 Application to ZnWO₄ crystal

Ab initio calculations of the structural and electronic properties of wolframite-type ZnWO₄ crystal have been performed within the periodic LCAO method using hybrid Hartree-Fock–DFT theory. The obtained results are in good agreement with known experimental data. Tungsten-oxygen chemical bonding is found to be highly covalent, whereas zinc-oxygen bonds have more ionic behavior. Calculated density of states is in good agreement with the experimental XPS spectrum from [19]. The main contribution to the valence band is due to the Zn 3*d* states at high binding energies and the O 2*p* and W 5*d* characters at low and medium binding energies.

The calculated phonon frequencies have been compared with the results of infrared and Raman spectroscopies. Rather good accuracy of ab initio phonon frequencies calculations makes them suitable for the prediction of the crystal vibrational properties especially in situations when the experimental approach is difficult or impossible due to selection rules.

Based on the crystal structure of ZnWO₄ and known properties, the three force-field (FF) models were constructed and potential parameters were optimized to give good agreement with structural properties, elastic constants and vibrational frequencies. The three FF models give reasonably good matching to the experimental properties. Next the MD simulations were performed for the three FF models, and the configuration

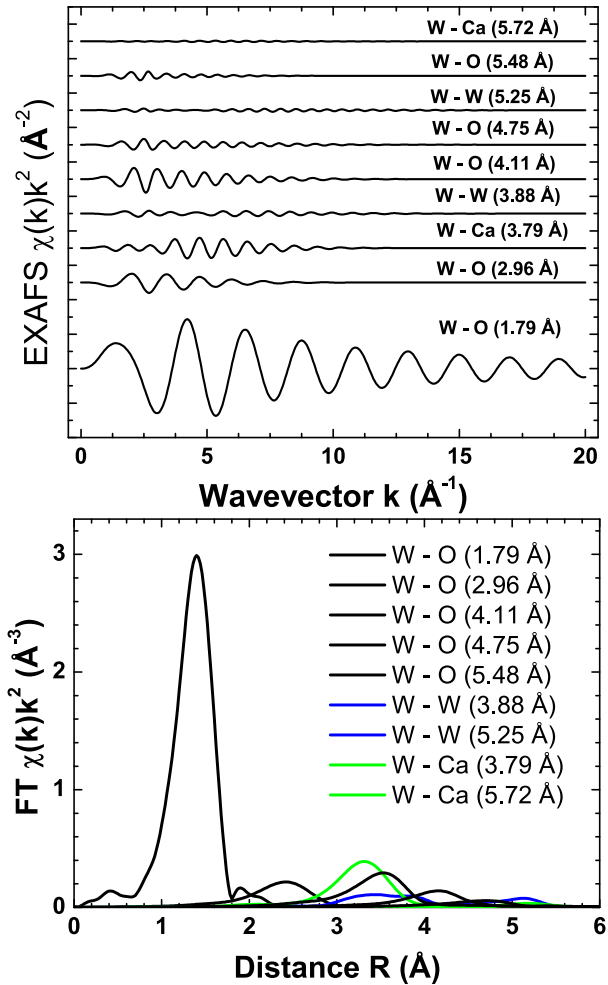


Figure 4.7: The W L_3 -edge EXAFS $\chi(k)k^2$ components for CaWO_4 in the single-scattering approximation and their Fourier transforms (FTs) corresponding to the atomic groups at different distances from the absorbing tungsten atom.

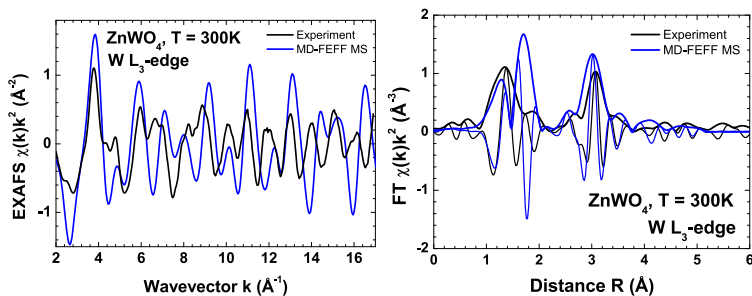


Figure 4.8: Results of EXAFS modelling using MD-EXAFS method for selected force-field model. (left panel) W L₃-edge EXAFS signal in ZnWO₄, (right panel) FT of the W L₃-edge EXAFS signal in ZnWO₄

averaged EXAFS signals were calculated. However, none of the calculated EXAFS signals gives good matching to the experimental signal (Fig. 4.8). The problem is that the developed FF models, based on simple pair potentials, cannot accurately describe the distorted structure of ZnWO₄, being due to the electronic Jahn-Teller effect. Therefore, more sophisticated simulation methods should be used, like reverse Monte-Carlo or ab initio molecular dynamics.

Conclusions

In this thesis the MD-EXAFS method for the EXAFS spectra modelling has been further developed based on the quantum mechanics-classical molecular dynamics (QMMD) approach coupled with ab initio EXAFS spectra calculations. The method expands possibilities in the interpretation of EXAFS spectra by accurate accounting of the thermal disorder within the multiple scattering effects. This allows one to obtain structural information contained beyond the first coordination shell on the many-atom distribution functions. In particular, the angles between chemical bonds and amplitudes of thermal vibrations including correlation effects can be determined.

The capability of the MD-EXAFS method has been demonstrated on an example of EXAFS spectra analysis for three polycrystalline compounds ReO_3 , CaWO_4 and ZnWO_4 , having different local coordinations. Besides, an example of the local structure determination in ZnWO_4 nanoparticles, based on the conventional EXAFS data analysis, is presented.

Besides the MD simulations, the quantum mechanical LCAO calculations have been also performed for ReO_3 , CaWO_4 and ZnWO_4 crystals. The self consistent procedure was used to find electronic structure and atomic charges. Then optimization of structural parameters was done and further different properties such as bulk modulus, phonon frequencies and phonon dispersion curves were calculated. Thus obtained physical properties were used during the force-field model optimization to increase the number of observables additionally to the experimentally available data.

In the case of ZnWO_4 nanoparticles the EXAFS spectra at the Zn K-edge and W L_3 -edge were measured and used in the analysis, allowing one to obtain information

on the local atomic structure around both absorbing atoms. It was found that strong relaxation of $[\text{ZnO}_6]$ and $[\text{WO}_6]$ octahedra occurs in nanoparticles comparing to the crystalline ZnWO_4 . While the interatomic W–O and Zn–O bond lengths show broad distribution already in the crystal, even shorter and longer bond lengths were found in nanoparticles. The possible explanation of this effect is structure relaxation and different distortion of the octahedra within single nanoparticle due to strong influence of the surface. The Raman spectra measurements allowed us to conclude that in nanoparticles short double W–O bonds are formed. This conclusion is based on the Raman frequency dependance from the bond length and correlates well with the appearance of short W–O distances in nanoparticles according to the EXAFS results.

ReO_3 , CaWO_4 and ZnWO_4 have different local coordination around $5d$ -element (W, Re): regular octahedra in ReO_3 , regular tetrahedra in CaWO_4 and strongly distorted octahedra in ZnWO_4 . Such difference in the local environment provides a good test of capabilities for the MD-EXAFS method. The structures with regular octahedra (ReO_3) and tetrahedra (CaWO_4) can be easily described by a force-field model based on the pair interatomic potentials. However, an additional three body potential is required for tetrahedral case to stabilize tetrahedral coordination during MD simulations. In the case of distorted octahedra (ZnWO_4) three force-field models of different complexity were developed which gave reasonable matching between calculated and experimental physical properties. Force-field models for all compounds were further used in molecular dynamics simulations.

The molecular dynamics allows one to introduce thermal atomic motion effects, and the temperature value is one of the simulation parameters. Because of the classical MD method used in the present work, the accurately accessible temperature region is limited to the high temperatures. In the present work, the lowest simulation temperature was set to 300 K for all compounds. In the case of ReO_3 the simulations were performed also at 423 K and 573 K.

As a result of MD simulations, sets of atomic configurations were obtained for each temperature and used to calculate the radial distribution functions, bond angle distributions and atomic movement trajectory determination. To check reliability of the MD simulations, the configuration-averaged EXAFS spectra were calculated and directly compared with the experimental ones.

The configuration-averaged EXAFS spectra for both compounds, ReO_3 and CaWO_4 , build from regular octahedra and tetrahedra units, respectively, show good agreement with the experimental EXAFS spectra. Also the temperature dependence of the EXAFS spectra for ReO_3 is well reproduced within the single force-field model. Therefore, we conclude that the force-field models describe rather accurately the thermal motion of atoms, including the correlation effects.

However, all developed force-field models for ZnWO_4 , having distorted $[\text{WO}_6]$ and $[\text{ZnO}_6]$ octahedra, did not provide good matching with the experimental EXAFS spectra. The reason of that is the nature of $[\text{WO}_6]$ octahedra distortion, which is caused by the second order Jahn-Teller effect: tungsten ions in ZnWO_4 have 6+ valence state and $5d^0$ electronic configuration, however some amount of electronic charge is back-transferred from the oxygen neighbours to the $5d$ states causing the removal of degeneracy by symmetry lowering. Such situation cannot be described accurately by simple pair potentials. However, the possible solution to this problem can be the use of the quantum molecular dynamics simulations. Such calculations nowadays are very time consuming and are possible mostly for small molecules. For simulation of the EXAFS spectra from crystals, hundreds or thousands atoms are usually required depending on the system, therefore the use of the quantum MD simulations is not practical today. However, the possibility to model such octahedra distortions has been confirmed by our quantum mechanical LCAO calculations for static ZnWO_4 structure.

The good agreement between the experimental and simulated EXAFS spectra for ReO_3 and CaWO_4 allowed us to make deeper analysis of their structure and atomic motion.

In ReO_3 the atomic motion trajectories show strong anisotropy of oxygen atoms vibrations, which are large perpendicular to the Re–O–Re bonds, thus resulting in a deviation of the Re–O–Re mean angle value from 180° to around 176° at 300 K and 174° at 573 K. The multiple-scattering effect contribution to the EXAFS spectra for the second and further coordination shells was analysed in details. It was found that the MS effects are responsible for about 50% drop of the Re L_3 -edge EXAFS signal amplitude in the second coordination shell and about 30% in the third coordination shell.

In CaWO_4 the multiple scattering effects are relatively small comparing to ReO_3 . The W L_3 -edge EXAFS spectrum was decomposed into components from different

groups of atoms. The main contribution comes from the nearest oxygens, while more distant atoms produce a signal being five and more times less in amplitude. The peaks in the Fourier transform of the EXAFS spectrum at 2.5 Å and 4.2 Å are due to oxygen atoms. The peak at 3.5 Å is composed of three contributions from O, Ca and W atoms.

In the future, the MD-EXAFS method can be applied to the materials with symmetrical local structure with the goal to extract additional information on the local dynamical structure from EXAFS spectra. Further improvements of the MD-EXAFS method are possible at the step of the potential parameters optimization by including additional observables as, for example, mean square relative displacements obtained from EXAFS conventional analysis. Moreover, the whole EXAFS spectrum may be used as an observable in the optimization procedure in the future. Another way to improve performance of the MD-EXAFS method is to use ab-initio MD instead of the classical one. This will allow one to deal with the materials having strong local distortions, like ZnWO_4 , as well as to extend applicability of the method to the low-temperatures region, where quantum effects dominate.

Main theses

1. The combined use of classical molecular dynamics and x-ray absorption spectra calculations from the first principles allows one to make accurate interpretation of the EXAFS spectra for crystalline compounds (ReO_3 and CaWO_4) taking into account the many-atoms distribution functions. This approach allows one to access the mean square relative displacements (EXAFS Debye-Waller factor) for atom pairs and the bonding angles distributions in outer coordination shells.
2. The vibrations of the oxygen atoms in ReO_3 structure are anisotropic, having the vibration amplitude along the Re–O–Re bonds direction smaller than that perpendicular to the Re–O–Re bonds. It is shown that the perpendicular oxygen vibrations lead to a decrease of the mean Re–O–Re angle value below 180° and to its weak temperature dependence.
3. The contribution from the single-scattering effects is dominating in the W L_3 -edge EXAFS spectrum of CaWO_4 . It is shown that oxygen atoms group at 2.96 \AA and calcium and oxygen groups at 3.79 \AA and 4.11 \AA , respectively, give the main contribution into the EXAFS signal beyond the first coordination shell.
4. The local atomic structure of ZnWO_4 nanoparticles around W and Zn atoms is noticeably deformed comparing to the microcrystalline powder. It is shown that the deformation of the $[\text{WO}_6]$ octahedra is related to the formation of the short ($\sim 1.74 \text{ \AA}$) double W=O bonds.

References

- [1] <http://www.hasyllab.de>. 18
- [2] N. D. AFIFY AND G. MOUNTJOY. **Molecular-dynamics modeling of Eu^{3+} -ion clustering in SiO_2 glass.** *Phys. Rev. B*, **79**:024202, 2009. 2
- [3] N. L. ALLAN, G. D. BARRERA, J. A. PURTON, C. E. SIMS, AND M. B. TAYLOR. **Ionic solids at elevated temperatures and or high pressures: lattice dynamics, molecular dynamics, Monte Carlo and ab initio studies.** *Phys. Chem. Chem. Phys.*, **2**:1099–1111, 2000. 1
- [4] A. L. ANKUDINOV, B. RAVEL, J. J. REHR, AND S. D. CONRADSON. **Real-space multiple-scattering calculation and interpretation of x-ray-absorption near-edge structure.** *Phys. Rev. B*, **58**:7565–7576, 1998. 15
- [5] A. ANSPOKS AND A. KUZMIN. **Interpretation of the Ni K-edge EXAFS in nanocrystalline nickel oxide using molecular dynamics simulations.** *J. Non-Cryst. Solids*, **357**(14):2604–2610, 2011. 10
- [6] D. CABARET, M. LE GRAND, A. RAMOS, A. M. FLANK, S. ROSSANO, L. GALOISY, G. CALAS, AND D. GHALEB. **Medium range structure of borosilicate glasses from Si K-edge XANES: a combined approach based on multiple scattering and molecular dynamics calculations.** *J. Non-Cryst. Solids*, **289**:1–8, 2001. 10
- [7] M. CHERGUI. **Picosecond and femtosecond X-ray absorption spectroscopy of molecular systems.** *Acta Crystallogr. A*, **66**(2):229–239, 2010. 2
- [8] A. DI CICCO, M. MINICUCCI, E. PRINCIPI, A. WITKOWSKA, J. RYBICKI, AND R. LASKOWSKI. **Testing interaction models by using x-ray absorption spectroscopy: solid Pb.** *J. Phys.: Condens. Matter*, **14**(12):3365, 2002. 10
- [9] T. G. COOPER AND N. H. DE LEEUW. **A combined ab initio and atomistic simulation study of the surface and interfacial structures and energies of hydrated scheelite: introducing a CaWO_4 potential model.** *Surf. Sci.*, **531**(2):159–176, 2003. 23

-
- [10] F. D'ACAPITO, S. MOBILIO, P. GASTALDO, D. BARBIER, L. F. SANTOS, O. MARTINS, AND R. M. ALMEIDA. **Local order around Er^{3+} ions in $\text{SiO}_2\text{-TiO}_2\text{-Al}_2\text{O}_3$ glassy films studied by EXAFS.** *J. Non-Cryst. Solids*, **293-295**(0):118–124, 2001. 2
- [11] G. FERLAT, A. SAN MIGUEL, J. F. JAL, J. C. SOETENS, PH. A. BOPP, I. DANIEL, S. GUILLOT, J. L. HAZEMANN, AND R. ARGOUT. **Hydration of the bromine ion in a supercritical 1:1 aqueous electrolyte.** *Phys. Rev. B*, **63**:134202, 2001. 2
- [12] A. FILIPPONI. **EXAFS for liquids.** *J. Phys.: Condens. Matter*, **13**(7):R23, 2001. 2
- [13] A. FILIPPONI AND A. DI CICCIO. **X-ray-absorption spectroscopy and n -body distribution functions in condensed matter. II. Data analysis and applications.** *Phys. Rev. B*, **52**:15135–15149, 1995. 3
- [14] A. FILIPPONI, A. DI CICCIO, AND C. R. NATOLI. **X-ray-absorption spectroscopy and n -body distribution functions in condensed matter. I. Theory.** *Phys. Rev. B*, **52**:15122–15134, 1995. 3
- [15] P. FORNASINI, F. MONTI, AND A. SANSON. **On the cumulant analysis of EXAFS in crystalline solids.** *J. Synchrotron Radiat.*, **8**(6):1214–1220, 2001. 9
- [16] B. FULTZ, T. KELLEY, J. D. LEE, M. AIVAZIS, O. DELAIRE, AND D. ABERNATHY. *Experimental Inelastic Neutron Scattering*. Springer-Verlag, 2004. 14
- [17] J. D. GRUNWALDT, C. KERESSZEGI, T. MALLAT, AND A. BAIKER. **In situ EXAFS study of $\text{Pd}/\text{Al}_2\text{O}_3$ during aerobic oxidation of cinnamyl alcohol in an organic solvent.** *J. Catal.*, **213**(2):291–295, 2003. 2
- [18] T. GUO. **More power to X-rays: New developments in X-ray spectroscopy.** *Laser Photonics Rev.*, **3**(6):591–622, 2009. 2
- [19] M. ITOH, N. FUJITA, AND Y. INABE. **X-Ray Photoelectron Spectroscopy and Electronic Structures of Scheelite- and Wolframite-Type Tungstate Crystals.** *J. Phys. Soc. Jpn.*, **75**(8), 2006. 24
- [20] F. JALILEHVAND, D. SPANGBERG, P. LINDQVIST-REIS, K. HERMANSSON, I. PERSSON, AND M. SANDSTRM. **Hydration of the Calcium Ion. An EXAFS, Large-Angle X-ray Scattering, and Molecular Dynamics Simulation Study.** *J. Am. Chem. Soc.*, **123**(3):431–441, 2001. 10
- [21] P. KIDKHUNTHOD AND A. C. BARNES. **A structural study of praseodymium gallate glasses by combined neutron diffraction, molecular dynamics and EXAFS techniques.** *J. Phys.: Conf. Series*, **190**(1):012076, 2009. 10
- [22] A. KUZMIN. **Application of cluster computing in materials science.** *Latvian J. Phys. Technol. Sci.*, **2**:7–14, 2006. 5

- [23] A. KUZMIN, G. DALBA, P. FORNASINI, F. ROCCA, AND O. SIPR. **X-ray absorption spectroscopy of strongly disordered glasses: Local structure around Ag ions in $g\text{-Ag}_2\text{O}\cdot n\text{B}_2\text{O}_3$.** *Phys. Rev. B*, **73**:174110, 2006. 2
- [24] A. KUZMIN, V. EFIMOV, E. EFIMOVA, V. SIKOLENKO, S. PASCARELLI, AND I.O. TROYANCHUK. **Interpretation of the Co K-edge EXAFS in LaCoO_3 using molecular dynamics simulations.** *Solid State Ionics*, **188**(1):21–24, 2011. 10
- [25] A. KUZMIN AND R. A. EVARESTOV. **Quantum mechanics-classical molecular dynamics approach to EXAFS.** *J. Phys.: Conf. Series*, **190**(1):012024, 2009. 10, 13
- [26] A. KUZMIN AND R. A. EVARESTOV. **Quantum mechanicsmolecular dynamics approach to the interpretation of x-ray absorption spectra.** *J. Phys.: Condens. Matter*, **21**(5):055401, 2009. 10, 13
- [27] A. KUZMIN, R. KALENDAREV, J. PURANS, J. P. ITIE, F. BAUDELET, A. CONGEDUTI, AND P. MUNSCH. **EXAFS study of pressure-induced phase transition in SrWO_4 .** *Phys. Scripta*, **2005**:556, 2005. 2
- [28] A. KUZMIN AND P. PARENT. **Focusing and superfocusing effects in X-ray absorption fine structure at the iron K edge in FeF_3 .** *J. Phys.: Condens. Matter*, **6**(23):4395, 1994. 12
- [29] A. KUZMIN AND J. PURANS. **Dehydration of the molybdenum trioxide hydrates $\text{MoO}_3 \cdot n\text{H}_2\text{O}$: in situ x-ray absorption spectroscopy study at the Mo K edge.** *J. Phys.: Condens. Matter*, **12**(9):1959, 2000. 9
- [30] R. LASKOWSKI, J. RYBICKI, M. CHYBICKI, AND A. DI CICCIO. **Pair Potential for Solid Rhodium from Extrapolated Ab-Initio Data.** *Phys. stat. sol. (b)*, **217**(2):737–746, 2000. 10
- [31] H. MATSUURA, S. WATANABE, H. AKATSUKA, Y. OKAMOTO, AND A. K. ADYA. **XAFS analyses of molten metal fluorides.** *J. Fluorine Chem.*, **130**(1):53–60, 2009. 10
- [32] P. J. MERKLING, A. MUNOZ-PAEZ, J. M. MARTINEZ, R. R. PAPPALARDO, AND E. SANCHEZ MARCOS. **Molecular-dynamics-based investigation of scattering path contributions to the EXAFS spectrum: The Cr^{3+} aqueous solution case.** *Phys. Rev. B*, **64**:012201, 2001. 10
- [33] B. MIERZWA. **EXAFS studies of bimetallic palladiumcobalt nanoclusters using Molecular Dynamics simulations.** *J. Alloy Compd.*, **401**:127–134, 2005. 10
- [34] G. MOUNTJOY. **Molecular dynamics, diffraction and EXAFS of rare earth phosphate glasses compared with predictions based on bond valence.** *J. Non-Cryst. Solids*, **353**:2029–2034, 2007. 10

- [35] M. A. NEWTON, A. J. DENT, AND J. EVANS. **Bringing time resolution to EXAFS: recent developments and application to chemical systems.** *Chem. Soc. Rev.*, **31**:83–95, 2002. 2
- [36] Y. OKAMOTO. **XAFS simulation of highly disordered materials.** *Nucl. Instrum. Meth. A*, **526**(3):572–583, 2004. 10
- [37] P. F. PETERSON, TH. PROFFEN, I. K. JEONG, S. J. L. BILLINGE, K. S. CHOI, M. G. KANATZIDIS, AND P. G. RADAELLI. **Local atomic strain in $\text{ZnSe}_{1-x}\text{Te}_x$ from high real-space resolution neutron pair distribution function measurements.** *Phys. Rev. B*, **63**:165211, 2001. 2
- [38] J. PURANS, G. DALBA, P. FORNASINI, A. KUZMIN, S. DE PANFILIS, AND F. ROCCA. **EXAFS and XRD Studies with Subpicometer Accuracy: The Case of ReO_3 .** *AIP Conference Proceedings*, **882**(1):422–424, 2007. 18
- [39] J. PURANS, J. TIMOSHENKO, A. KUZMIN, G. DALBA, P. FORNASINI, R. GRISENTI, N. D. AFIFY, F. ROCCA, S. DE PANFILIS, I. OZHOGIN, AND S. I. TIUTIUNNIKOV. **Femtometer accuracy EXAFS measurements: Isotopic effect in the first, second and third coordination shells of germanium.** *J. Phys.: Conf. Series*, **190**(1):012063, 2009. 3
- [40] J. J. REHR AND R. C. ALBERS. **Theoretical approaches to x-ray absorption fine structure.** *Rev. Mod. Phys.*, **72**(3):621–654, 2000. 2, 3, 15
- [41] H. M. RIETVELD. **A profile refinement method for nuclear and magnetic structures.** *J. Appl. Crystallogr.*, **2**(2):65–71, 1969. 1
- [42] O. M. ROSCIONI, N. ZONIAS, S. W. T. PRICE, AN. E. RUSSELL, T. COMASCHI, AND C. K. SKYLARIS. **Computational prediction of L_3 EXAFS spectra of gold nanoparticles from classical molecular dynamics simulations.** *Phys. Rev. B*, **83**(11):115409, 2011. 10
- [43] S. ROSSANO, A. RAMOS, J.-M. DELAYE, S. CREUX, A. FILIPPONI, CH. BROUDER, AND G. CALAS. **EXAFS and Molecular Dynamics combined study of CaO-FeO-2SiO_2 glass. New insight into site significance in silicate glasses.** *Europhys. Lett.*, **49**(5):597, 2000. 10
- [44] A. SANSON. **Local dynamical properties of crystalline germanium and their effects in extended x-ray absorption fine structure.** *Phys. Rev. B*, **81**:012304, 2010. 10
- [45] A. SENYSHYN, H. KRAUS, V. B. MIKHAILIK, AND V. YAKOVYNA. **Lattice dynamics and thermal properties of CaWO_4 .** *Phys. Rev. B*, **70**(21):214306, 2004. 23

-
- [46] R. SPEZIA, M. DUVAİL, P. VITORGE, T. CARTAILLER, J. TORTAJADA, G. CHILLEMI, P. DANGELO, AND M. P. GAIGEOT. **A Coupled Car-Parrinello Molecular Dynamics and EXAFS Data Analysis Investigation of Aqueous Co^{2+} .** *J. Phys. Chem. A*, **110**(48):13081–13088, 2006. 10
- [47] R. SPEZIA, M. DUVAİL, P. VITORGE, AND P. D'ANGELO. **Molecular dynamics to rationalize EXAFS experiments: A dynamical model explaining hydration behaviour across the lanthanoid(III) series.** *J. Phys.: Conf. Series*, **190**(1):012056, 2009. 10
- [48] J. TIMOSHENKO, A. KUZMIN, AND J. PURANS. **Molecular dynamics simulations of EXAFS in germanium.** *Cent. Eur. J. Phys.*, **9**:710–715, 2011. 10
- [49] A. WITKOWSKA, J. RYBICKI, AND A. DI CICCIO. **Structure of partially reduced bismuthsilicate glasses: EXAFS and MD study.** *J. Alloy Compd.*, **401**:135–144, 2005. 10
- [50] A. WITKOWSKA, J. RYBICKI, AND A. DI CICCIO. **Structure of partially reduced $x\text{PbO} (1-x)\text{SiO}_2$ glasses: combined EXAFS and MD study.** *J. Non-Cryst. Solids*, **351**(5):380–393, 2005. 10
- [51] A. WITKOWSKA, J. RYBICKI, S. DE PANFILIS, AND A. DI CICCIO. **The structure of liquid lead: EXAFS and MD studies.** *J. Non-Cryst. Solids*, **352**:4351–4355, 2006. 10
- [52] K. YAGI, S. UMEZAWA, H. TERAUCHI, AND H. KASATANI. **EXAFS study of phase transitions in KIO_3 .** *J. Synchrotron Radiat.*, **8**(2):803–805, 2001. 2

Author's publication list

1. A. Kalinko, A. Kuzmin, R.A. Evarestov, **Ab initio study of the electronic and atomic structure of the wolframite-type ZnWO_4** , Solid State Commun. 149 (2009) 425-428.
2. A. Kalinko, A. Kuzmin, **Raman and photoluminescence spectroscopy of zinc tungstate powders**, J. Lumin. 129 (2009) 1144-1147.
3. R. A. Evarestov, A. Kalinko, A. Kuzmin, M. Losev, J. Purans, **First-principles LCAO calculations on 5d transition metal oxides: electronic and phonon properties**, Integr. Ferroelectrics 108 (2009) 1-10.
4. A. Kalinko, R. A. Evarestov, A. Kuzmin, J. Purans, **Interpretation of EXAFS in ReO_3 using molecular dynamics simulations**, J. Phys.: Conf. Ser. 190 (2009) 012080.
5. A. Kalinko, A. Kuzmin, **Static and dynamic structure of ZnWO_4 nanoparticles**, J. Non-Cryst. Solids 357 (2011) 2595-2599.
6. A. Kalinko, A. Kotlov, A. Kuzmin, V. Pankratov, A.I. Popov, L. Shirmane, **Electronic excitations in ZnWO_4 and $\text{Zn}_x\text{Ni}_{1-x}\text{WO}_4$ ($x=0.1-0.9$) using VUV synchrotron radiation**, Cent. Eur. J. Phys. 9 (2011) 432-437.
7. A. Kuzmin, A. Kalinko, R.A. Evarestov, **First-principles LCAO study of phonons in NiWO_4** , Cent. Eur. J. Phys. 9 (2011) 502-509.

Participation in conferences

1. A. Kalinko, A. Kuzmin, **Raman and photoluminescence spectroscopy of zinc tungstate powders**, International Baltic Sea Region Conference 'Functional Materials and Nanotechnologies' (FM&NT), 2008, Riga, Latvia
2. A. Kalinko, A. Kuzmin, R.A. Evarestov **Ab initio study of the electronic and atomic structure of the wolframite-type ZnWO_4** , International Baltic Sea Region Conference 'Functional Materials and Nanotechnologies' (FM&NT), 2008, Riga, Latvia
3. A. Kalinko, A. Kuzmin, R.A. Evarestov **Electronic structure calculations of ZnWO_4 : periodic and nanocluster models**, 6th International Conference on Advanced Optical Materials and Devices (AOMD-6), 2008, Riga, Latvia
4. A. Kalinko, A. Kuzmin, **Molecular dynamics simulations of ReO_3** ISSP 25th Scientific Conference, 2009, Riga, Latvia
5. A. Kalinko, R.A. Evarestov, A. Kuzmin, M. Losev, J. Purans, **Structural, Electronic and Phonon Properties of Metallic ReO_3** , International Baltic Sea Region Conference 'Functional Materials and Nanotechnologies' (FM&NT), 2009, Riga, Latvia
6. A. Kalinko, A. Kuzmin, R.A. Evarestov **First Principles LCAO Calculations of Tungstates MeWO_4 (Me = Ca, Mg, Zn)**, International Baltic Sea Region Conference 'Functional Materials and Nanotechnologies' (FM&NT), 2009, Riga, Latvia

7. A. Kalinko, R.A. Evarestov, A. Kuzmin, J. Purans, **Interpretation of EXAFS From ReO_3 Using Molecular Dynamics Simulations**, 14th International Conference on X-ray Absorption Fine Structure (XAFS14), 2009, Camerino, Italy
8. A. Kalinko, A. Kuzmin, **Determining crystal structure and atomic positions using EXAFS** ISSP 26th Scientific Conference, 2010, Riga, Latvia
9. A. Kalinko, J. Timoshenko, A. Kuzmin, **EXAFS study of ZnWO_4 on the W L_3 and Zn K edges**, International Baltic Sea Region Conference 'Functional Materials and Nanotechnologies' (FM&NT), 2010, Riga, Latvia
10. A. Kalinko, A. Kuzmin, **Static and Dynamic Structure of ZnWO_4 Nanoparticles**, 11th International Conference on the Structure of Non-Crystalline Materials (NCM11), 2010, Paris, France
11. A. Kalinko, A. Kuzmin, **Crystal Structure Determination Using EXAFS Total Scattering Phase**, International Baltic Sea Region Conference 'Functional Materials and Nanotechnologies' (FM&NT), 2011, Riga, Latvia

Participation in schools with posters

1. A. Kalinko, A. Kuzmin, R.A. Evarestov, **Electronic and Atomic Structure Study of ZnWO_4** , Nordic and European Summer School "VUV and X-ray Research for the Future using FEL's and Ultra Brilliant Sources", May 26 - June 2, 2008, Odengarden and MAX-lab, Sweden
2. A. Kalinko, A. Kuzmin, R.A. Evarestov, **Molecular Dynamics Approach to Calculation of EXAFS Spectra**, CCP5 Methods in Molecular Simulation Summer School, July 06-15, 2008, Sheffield, UK
3. A. Kalinko, A. Kuzmin, **Zinc Tungstate Powders Investigation by Spectroscopic Methods**, 7th PSI Summer School on Condensed Matter Research, August 15-23, 2008, ZuoZ, Switzerland
4. A. Kalinko, A. Kuzmin, **Interpretation of x-ray absorption spectra using molecular dynamics simulations**, Higher European Research Course for Users of Large Experimental Systems (HERCULES 2011), February 27 - March 31, 2011, Grenoble and Paris, France

Acknowledgements

I am grateful to my supervisor Dr. Alexei Kuzmin who guided me during the whole period of my PhD studies and provided great atmosphere for our scientific research. I would like to thank Prof. Robert A. Evarestov for invaluable help in understanding the art of the quantum chemistry calculations. I would also thank Dr. Juris Purans for his helpful discussions and advices throughout the research.

I would also like to extend my thanks to Dr. Larisa Grigorjeva for providing all the facilities needed for the photoluminescence and infra-red spectra measurements.

I would to express gratitude to my parents for their encouragement and support over the many years of my studies.